Influence of Metallic Precursors on the Preparation of Silica-Supported PtSn Alloy: Characterization and Reactivity in the Catalytic Activation of CO_2

Jordi Llorca,* Pilar Ramírez de la Piscina,* José-Luis G. Fierro,† Joaquim Sales,* and Narcís Homs*

*Departament de Química Inorgànica, Universitat de Barcelona, Diagonal 647, 08028 Barcelona, Spain; and †Instituto de Catálisis y Petroleoquímica, C.S.I.C., Cantoblanco, 28049 Madrid, Spain

The preparation of a single, well-defined PtSn phase supported on silica was carried out by the definitive interaction of cis-[PtCl$_2$(PPh$_3$)$_2$] and SnCl$_2$ with the hydroxyl surface groups of silica. After a reduction step, the only metallic phase present on the catalyst was the supported PtSn alloy, which was unambiguously characterized by X-ray diffraction, transmission electron microscopy, energy dispersive X-ray analysis, electron nanodiffraction, and X-ray photoelectron spectroscopy. Its structural properties and improved catalytic behaviour in the CO_2 reaction with C_2H_4 and H_2 or H_2O are contrasted with those of a conventional catalyst prepared from H_2PtCl_6 and SnCl$_2$. © 1995 Academic Press, Inc.

INTRODUCTION

There is current interest in the activation of the CO_2 molecule and its utilization as a feedstock in chemical transformations. The present work describes a new route for the catalytic activation of CO_2 in which ethylene is used, involving the selective synthesis in the heterogeneous phase over PtSn alloy supported on silica of a useful organic compound with a new C–C bond. Many studies describe the preparation and characterization of platinum–tin supported catalysts due to their application in various areas of catalysis (1–6). However, their characterization has not always been achieved unambiguously, and the difficulty of preparing only one well-defined Pt–Sn supported phase has been established (7–11). Due to the complexity of these Pt–Sn systems, in which several mono- or bimetallic phases may coexist, it is difficult to relate their catalytic properties with their structural characteristics and the various metallic phases formed. Thus, the development of new methods to prepare Pt–Sn supported catalysts is a subject of current interest.

The heterogenization of coordination compounds through a definitive interaction with the functional groups of a support can produce unique surface species, which can be transformed into new and well-defined metallic phases under appropriate conditions. We have studied the heterogenization of several platinum and tin compounds (12–14).

Here we report the preparation of a catalyst which has only the well-defined PtSn alloy supported on silica. We show its unambiguous characterization by X-ray diffraction (XRD), transmission electron microscopy (TEM), energy dispersive X-ray analysis (EDX), electron nanodiffraction, and X-ray photoelectron spectroscopy (XPS). In addition, we demonstrate its activity in the catalytic reaction between carbon dioxide, ethylene, and hydrogen or water. The catalytic performance and structural characteristics of this catalyst have been compared with another PtSn catalyst prepared by a conventional method from H_2PtCl_6 and SnCl$_2$.

EXPERIMENTAL

Preparation of Catalysts

The support used was a Degussa Aerosil-type silica with a BET surface area of 200 m^2 g^{-1} and a low impurity content. All chemicals used were of analytical reagent grade. Solvents were distilled, kept under argon, and stored over activated molecular sieves. The complex cis-[PtCl$_2$(PPh$_3$)$_2$] was prepared and characterized according to literature methods (15).

For the preparation of catalysts, the support was first dehydrated by treatment under high vacuum at 473 K for 16 h. The preparation was carried out in two steps. First, platinum was incorporated from a methylene chloride solution of cis-[PtCl$_2$(PPh$_3$)$_2$] or an acetone solution of H_2PtCl_6. The system was treated under vacuum at 373 K overnight and then tin was incorporated into the catalyst from an acetone solution of SnCl$_2$. Samples were prepared with a 3% platinum loading and a molar ratio Sn/Pt = 1. After impregnation, samples were dried under high vacuum at 373 K for 16 h and then reduced with hydrogen flow (40
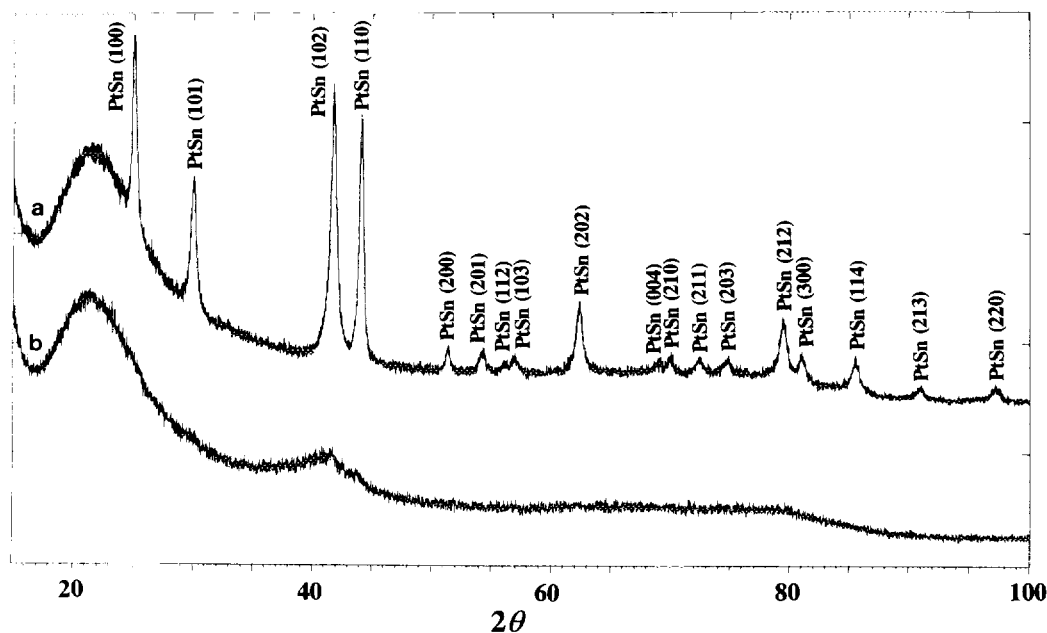
FIG. 1. XRD patterns of silica-supported Pt–Sn catalysts. (a) Pt(PPh₃)–Sn/Si catalyst; (b) PtCl–Sn/Si catalyst. The broad signal centered at $2\theta = 21°$ is due to the anomalous silica diffraction.

ml min⁻¹) at 673 K for 16 h. The respective [PtCl₂(PPh₃)₂]/ SnCl₂/SiO₂ and H₂PtCl₆/SnCl₂/SiO₂ catalysts obtained are referred to as Pt(PPh₃)–Sn/Si and PtCl–Sn/Si, depending on the metallic precursor used in the preparation.

Two catalysts, with a 3% platinum loading, were prepared following a similar procedure with only platinum in the active phase. After platinum incorporation the samples were similarly dried and reduced. The resulting catalysts are also referred to as Pt(PPh₃)/Si and PtCl/Si, respectively.

Catalyst Characterization

The XRD profiles were collected at a step width of 0.02 degrees and by counting 10 s at each step in the 2θ range of interest using a Siemens D-500 X-ray diffractometer equipped with a graphite monochromator and a Cu target. The average particle size was estimated by using the Scherrer formula at various high-intensity reflections corrected from CuKα2 radiation.

Samples for TEM study were suspended in methanol and continuously stirred in an ultrasonic bath. The resulting suspensions were placed on carbon-coated copper grids and the alcohol was evaporated to obtain films of catalyst particles. EDX measurements were carried out in STEM mode using a Hitachi H 800-MT transmission electron microscope operating at 175 keV with a Kevex 8000 Quantum System. The X-rays emitted upon electron irradiation were acquired in the range 0–10 keV. The electron diffrac-
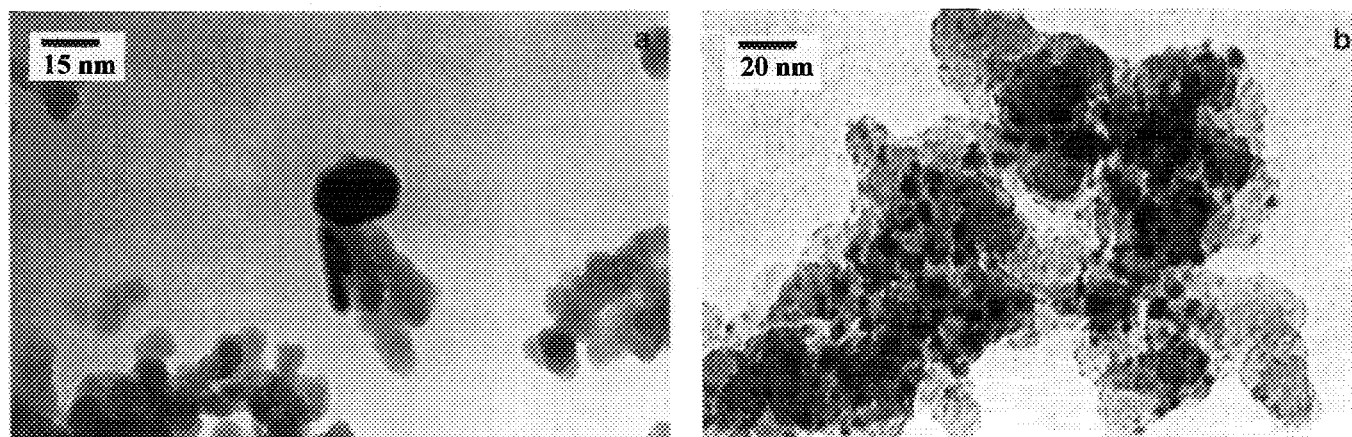

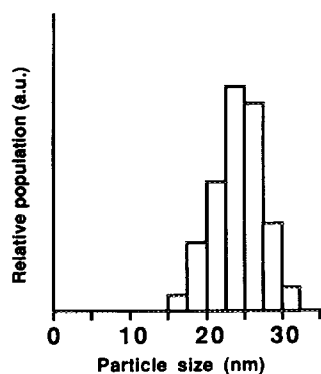FIG. 2. TEM micrograph of silica-supported Pt–Sn catalysts. (a) Pt(PPh₃)–Sn/Si catalyst; (b) PtCl–Sn/Si catalyst.

FIG. 3. Particle size distribution histogram obtained from TEM for PtSn alloy particles on silica corresponding to the Pt(PPh₃)–Sn/Si catalyst (more than 200 particles were used).

tion studies were carried out using a Hitachi H 800-NA transmission electron microscope operating in the convergent beam mode (CBED) at 200 keV with a 2–5 nm probe.

Photoelectron spectra were recorded with a Fisons ESCALAB Mk II 200R spectrometer equipped with a MgKα X-ray source ($h\nu = 1253.6$ eV) and a hemispherical electron analyzer. The X-ray source was operated at 12 kV and 10 mA. As an internal standard of the catalysts a binding energy of 284.9 eV was taken for the C 1s peak, which always gave a constant value for the Si 2p peak at 103.4 eV. The accuracy of the binding energy was within 0.2 eV. The samples were mounted onto a manipulator which allowed the transfer from the pretreatment chamber into the analysis chamber. All samples were treated in situ before XPS experiments in the pretreatment chamber at 673 K under hydrogen.

Catalytic Activity

Catalytic reaction was carried out in a stainless steel microreactor operating under continuous flow and differential conditions. High purity C_2H_4, CO_2, and H_2 were supplied from a pressurized manifold via individual mass flow controllers. H_2O was introduced into the reactant mixture by a mechanical pump equipped with a "var-ispeed" device that allowed the introduction of 0.067 ml H_2O min⁻¹. The reaction pressure was maintained by means of a back-pressure regulator, in the range 25 to 35 bar.

Reaction products were analyzed by on-line gas chromatography using a 3400 Varian GC equipped with an automated gas sample valve. A DB5 column, 60 m long, 0.32 mm i.d., connected to a flame ionization detector and a Hayesep column 6 m long, 2.16 mm i.d., and a 5Å molecular sieve column 0.9 m long 2.16, mm i.d. connected to a thermocouple detector were used to analyze the reaction products. The transfer line between the reactor and the chromatograph and all valves in the chromatograph were coated with fused silica and kept above 423 K to eliminate any product loss due to absorption and/or condensation. A complete analysis of the products was made by collecting them in a solid CO_2 trap at the reactor outlet and analyzing them by GC-MS using a Hewlett Packard 5971 mass selective detector.

RESULTS AND DISCUSSION

Characterization of Catalysts

The catalysts were characterized by XRD, TEM, EDX, and XPS techniques. In Fig. 1 the XRD patterns corre-
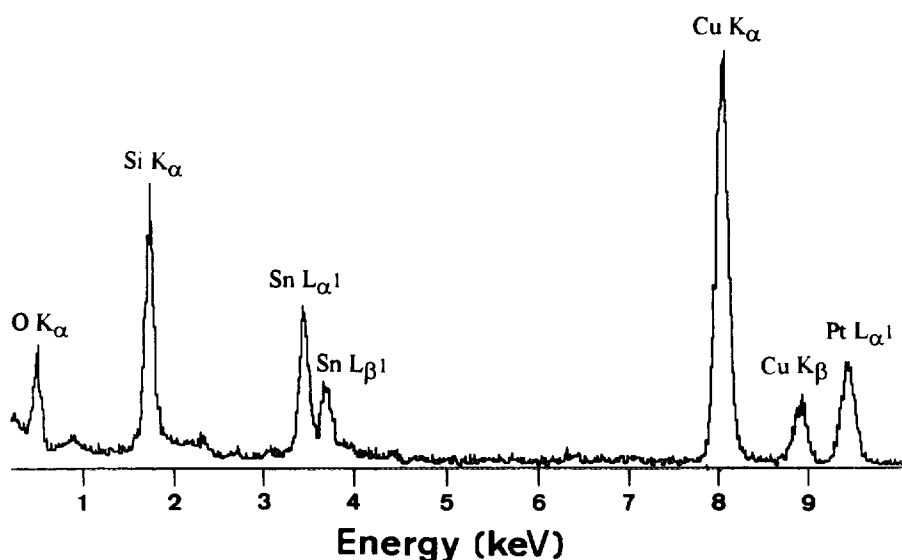

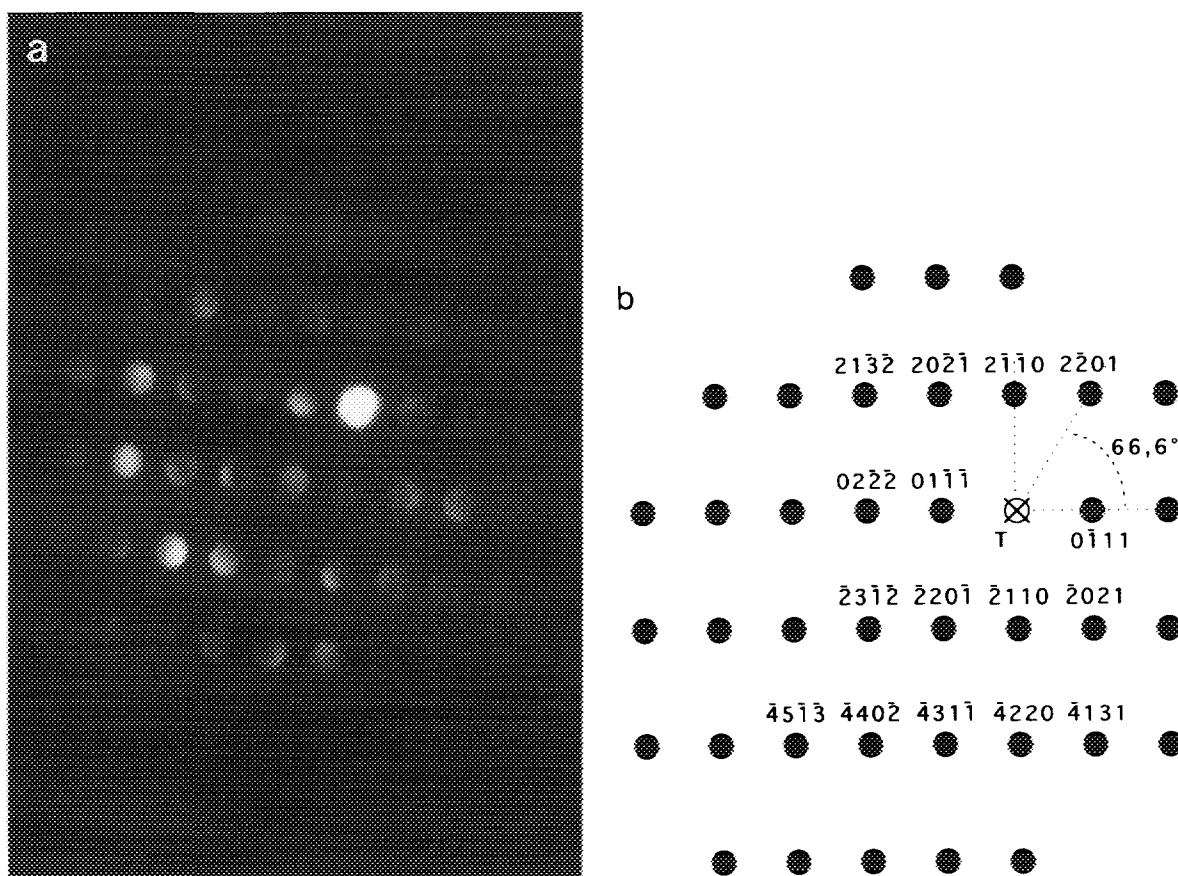FIG. 4. EDX pattern from a representative 25-nm particle of the Pt(PPh₃)–Sn/Si catalyst.

a

b

21̄32̄ 202̄1̄ 21̄1̄0 22̄01

66,6°

022̄2̄ 011̄1̄

T   01̄11

2̄31̄2̄ 2̄201̄ 2̄110 2̄021

4̄51̄3̄ 4̄402̄ 4̄311̄ 4̄220 4̄131

FIG. 5. (a) Electron nanodiffraction pattern from a representative individual particle of the $Pt(PPh_3)$–Sn/Si catalyst. The pattern shows that the particle has the PtSn (hcp) structure oriented in the [011̄2] crystallographic direction. (b) Indexed nanodiffraction pattern shown in (a).

sponding to the catalysts $Pt(PPh_3)$–Sn/Si and PtCl–Sn/Si are shown. The pattern of $Pt(PPh_3)$–Sn/Si (Fig. 1a) corresponds well to the presence of only hcp PtSn alloy, and no other mono- or bimetallic phase is observed; from the pattern a basal plane orientation of the platelets per-

TABLE 1

Binding Energies (eV) of Core Electrons, XPS Intensity Ratios, and XPS Atomic Ratios for the Silica-Supported Platinum Catalysts[a]

Catalyst	Pt $4f_{7/2}$	I_{Pt}/I_{Si}	I_{Sn}/I_{Si}	Pt/Sn	Sn^0/Sn
$Pt(PPh_3)$–Sn/Si	71.2	0.082	0.072	1.10	0.60
PtCl–Sn/Si	71.5	0.084	0.175	0.47	0.70
$Pt(PPh_3)$/Si	71.3	0.082	—	—	—
PtCl/Si	71.5	0.132	—	—	—

[a] The C 1s peak at a binding energy of 284.9 eV was taken as an internal standard. A value of 103.4 eV was obtained for the Si 2p peak in all experiments.

pendicular to the [001] direction can be inferred. In contrast, the XRD diffraction pattern of PtCl–Sn/Si (Fig. 1b) cannot be unambiguously assigned to any mono- or bimetallic phase.

The transmission electron micrograph of the $Pt(PPh_3)$–Sn/Si catalyst (Fig. 2a) shows only hexagonal particles homogeneously dispersed on silica, having a plate-like shape with about 6 nm height. Figure 3 displays their size distribution along the basal plane. It can be seen that they have a narrow size distribution about 24 nm in diameter. EDX patterns obtained for individual particles confirmed their bimetallic nature and showed for all of them the same composition (see Fig. 4). Electron nanodiffraction patterns of some of these particles were also feasible (see Fig. 5), and in all cases after a careful indexation the (hcp) PtSn alloy structure was established. On the other hand, for the PtCl–Sn/Si catalyst a representative TEM micrograph is shown in Fig. 2b. From this figure a preferential shape for the metallic particles cannot be distinguished. Moreover, EDX gave a different composition for different particles analyzed.

XP spectra of the catalysts corresponding to Si 2p, Pt

Sn $3d_{5/2}$ peaks relative to the Si $2p$ peak; from these data and the sensitivity factors according to Wagner *et al.* (16), the relative atomic ratios on the surface have been calculated. For the Pt(PPh₃)–Sn/Si catalyst the XPS Pt/Sn ratio is 1.1, close to the ratio expected for the PtSn alloy supported on silica, while the PtCl–Sn/Si catalyst shows a lower Pt/Sn ratio (0.47).

From all these results, the homogeneous characteristics of the Pt(PPh₃)–Sn/Si catalyst can be inferred; in this catalyst only the well-defined PtSn alloy is present on the silica support. The homogeneous characteristics of this catalyst contrast with those of the PtCl–Sn/Si counterpart, which was less defined and contains various metallic phases.

In order to compare the structure of catalysts containing platinum alone prepared from the different precursors, two Pt samples were prepared by impregnation of [PtCl₂(PPh₃)₂] and H₂PtCl₆ precursors and then reduced in H₂ flow at 673 K. Some differences can be established between these two samples. The XRD pattern shows a platinum phase on silica for the PtCl/Si catalyst with platinum particles with a diameter of about 2.5 nm (see Fig. 7). For the Pt(PPh₃)/Si catalyst no metallic phase was detected from the XRD pattern, probably due to the very small size of platinum particles in this case. Nevertheless, when the XRD pattern corresponding to the SiO₂ support used was subtracted, the Pt(111) reflection was observed (Fig. 7c). In fact for this catalyst the TEM micrograph shows small platinum particles highly dispersed on silica, smaller than those of the PtCl/Si sample (see Fig. 8). In both cases
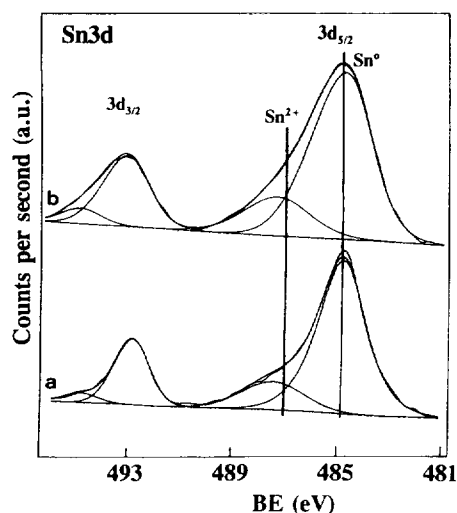

FIG. 6. Sn $3d$ core level spectra of silica-supported Pt–Sn catalysts. (a) Pt(PPh₃)–Sn/Si catalyst; (b) PtCl–Sn/Si catalyst.

$4f$, Sn $3d$, and Cl $2p$ levels have been recorded. No evidence for the presence of chlorine species on the surface by means of XPS was found in any case. The binding energies of Pt $4f_{7/2}$ peaks indicate the presence in all cases of reduced platinum (Pt⁰) species (see Table 1). The XP spectra of the Sn $3d$ level are shown in Fig. 6; a line-profile analysis through a peak deconvolution shows the presence of Sn⁰ and oxidized species of tin (see the Sn⁰/Sn_total ratio in Table 1). Table 1 also compiles the intensities of the Pt $4f_{7/2}$ and
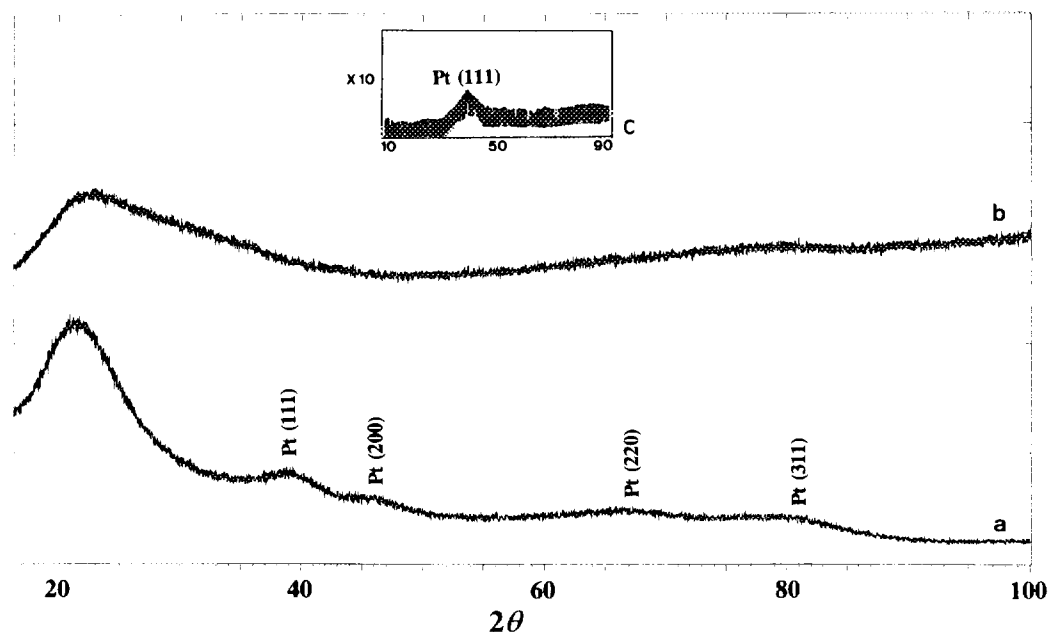

FIG. 7. XRD patterns of silica-supported Pt catalysts. (a) PtCl/Si catalyst; (b) Pt(PPh₃)/Si catalyst; (c) Pattern (b) after substraction of SiO₂ support pattern.
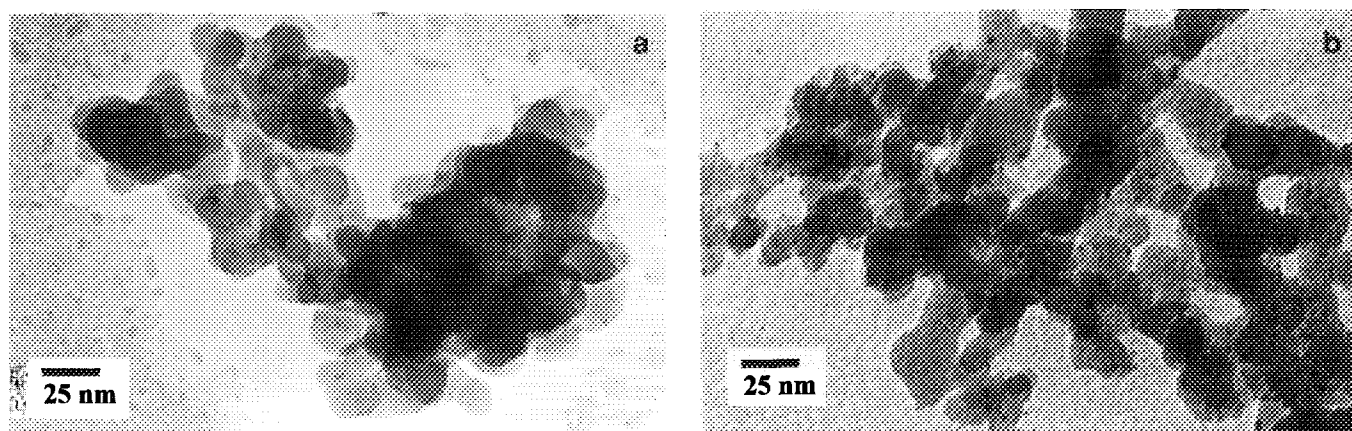
FIG. 8. TEM micrographs of silica-supported Pt catalysts. (a) Pt(PPh₃)/Si catalyst; (b) PtCl/Si catalyst.

XP spectra show the presence of Pt^0 on the surface (see Table 1).

These findings indicate that in the preparation of silica-supported PtSn catalysts the incorporation of platinum onto the silica is a very important step. Since the platinum precursor determines the characteristics of the final catalyst, the initial platinum surface species has a strong influence on the tin impregnation process. Probably in the catalyst prepared from [PtCl₂(PPh₃)₂] and SnCl₂ · CH₃COCH₃, an incipient but definite Pt–Sn interaction in the initial surface species after the impregnation step is responsible for the formation after the reduction step of only the PtSn phase.

Catalytic Activity

The catalytic reaction between CO₂ and C₂H₄ has been studied in the presence of hydrogen or water. In both cases, the only product obtained with a new C–C bond was lactic acid.

The results obtained in the presence of hydrogen are shown in Table 2. In this case, besides lactic acid, ethane and CO were produced. For the Pt(PPh₃)–Sn/Si catalyst the reaction was studied between 373 and 473 K, at 35 bar. The increase in the reaction temperature caused an increase in the rate of lactic acid production from 373 to 423 K; simultaneously a slight C₂H₄ hydrogenation was observed. However, at 473 K there was negligible lactic acid production and an increase in the C₂H₄ hydrogenation was found.

For comparative purposes, the PtCl–Sn/Si and PtCl/Si catalysts prepared by a conventional method were tested under the experimental conditions which yielded the highest production of lactic acid on the Pt(PPh₃)–Sn/Si catalyst. Negligible lactic acid production and significant C₂H₄ hydrogenation was observed on the PtCl–Sn/Si catalyst, whereas only C₂H₄ hydrogenation was found on the PtCl/Si counterpart.

For the lactic acid production from CO₂ and C₂H₄ in

TABLE 2

Catalytic Results of the Reaction among CO₂, C₂H₄, and H₂ over Several Silica-Supported Platinum Catalysts[a]

Catalyst	F/W[b] (ml/min/g cat.)	CO₂:C₂H₄:H₂ molar ratio	T (K)	CH₃CHOHCOOH (μmol/min/g cat.)	C₂H₆/C₂H₄ (%)
Pt(PPh₃)–Sn/Si	11	5:5:1	373	5	2
Pt(PPh₃)–Sn/Si	11	5:5:1	393	23.4	2
Pt(PPh₃)–Sn/Si	11	5:5:1	423	30.0	3
Pt(PPh₃)–Sn/Si	11	5:5:1	473	1.0	14
Pt(PPh₃)–Sn/Si	22	5:5:1	393	2.8	3
PtCl–Sn/Si	11.5	5:5:1	423	1.1	12
PtCl/Si	13.5	5:5:1	423	0	13

[a] Total pressure 35 bar.
[b] F and W are the flow rate and catalyst weight, respectively.

TABLE 3

Catalytic Activity in the Reverse Water–Gas Shift Reaction of Several Silica-Supported Platinum Catalysts[a]

Catalyst	F/W (ml/min/g catalyst)	CO (μmol/min/g catalyst)	H_2O
Pt(PPh₃)–Sn/Si	24	52	Detected
PtCl–Sn/Si	25	51	Detected
PtCl/Si	30	28	Not detected

[a] Reaction temperature 423 K, molar ratio $CO_2/H_2 = 1/1$.

the presence of H_2, an induction time was necessary during which the simultaneous appearance of CO and H_2O was found. After the induction time no H_2O was detected as a reaction product and lactic acid appeared. This behaviour led us to study the reverse of the water–gas shift (RWGS) reaction over the catalysts at representative reaction conditions. Results are shown in Table 3. The Pt(PPh₃)–Sn/Si and PtCl–Sn/Si catalysts were active in the RWGS reaction but in the case of PtCl/Si only CO was detected as a reaction product.

These findings point to the existence of two consecutive reactions [1] and [2] when CO_2 reacts with C_2H_4 and H_2:

$$CO_2 + H_2 \rightarrow CO + H_2O \quad [1]$$

$$CO_2 + C_2H_4 + H_2O \rightarrow CH_3CHOHCOOH. \quad [2]$$

Although both the Pt(PPh₃)–Sn/Si and the PtCl–Sn/Si catalysts were active in the RWGS reaction (see Table 3), only the former was able to give the reaction between CO_2 and C_2H_4 in the presence of formed water (see Table 2). This catalytic performance can be related to the homogeneous structural characteristics of the Pt(PPh₃)–Sn/Si catalyst in which only the well-defined PtSn alloy supported on silica is present as large monocrystalline platelets. On the other hand, when only CO_2 and C_2H_4 were supplied over the Pt(PPh₃)–Sn/Si catalyst at 423 K and 35 bar lactic acid and CO appeared at initial reaction times, then both disappeared and no products were further detected. This indicates that reactions [1] and [2] take place at initial reaction times when chemisorbed hydrogen from the reduction step is present.

In order to study the water-assisted CO_2 coupling to the mono-olefin the catalytic reaction between CO_2 and C_2H_4 in the presence of H_2O has been studied between 25 and 35 bar total pressure and at temperatures between 373 and 473 K. Table 4 compiles the results, which show for the catalyst Pt(PPh₃)–Sn/Si an increase in the catalytic activity with an increase in total pressure and with temperatures up to 423 K. The maximum activity was achieved at 423 K

TABLE 4

Catalytic Activity in the Production of Lactic Acid from CO_2, C_2H_4, and H_2O for Several Silica-Supported Platinum Catalysts[a]

Catalyst	F/W[b]	T (K)	Total pressure (bar)	CH₃CHOHCOOH (μmol/min/g catalyst)
Pt(PPh₃)–Sn/Si	140	373	35	1
Pt(PPh₃)–Sn/Si	140	393	35	27.8
Pt(PPh₃)–Sn/Si	140	423	25	2.8
Pt(PPh₃)–Sn/Si	140	423	30	38.8
Pt(PPh₃)–Sn/Si	140	423	35	109.3
Pt(PPh₃)–Sn/Si	140	473	35	6.8
PtCl–Sn/Si	146	423	35	0
PtCl/Si	173	423	35	0

[a] Molar ratio $CO_2:C_2H_4:H_2O = 1:1:1$.
[b] ml($CO_2 + C_2H_4$)min⁻¹/g catalyst.

and 35 bar. At this pressure an increase in the temperature to 473 K produced a significant decrease in the lactic acid production; this effect was also observed when the reaction was carried out in the presence of hydrogen. Conventional catalysts PtCl–Sn/Si and PtCl/Si were tested in the experimental conditions of maximum activity and no lactic acid was detected in any case. Pt(PPh₃)/Si was also inactive.

CONCLUSIONS

A unique and well-defined PtSn alloy supported on silica can be prepared by the two-step impregnation of cis-[PtCl₂(PPh₃)₂] and SnCl₂ metal precursors. The unambiguously determined structural characteristics of the catalyst prepared from these precursors strongly contrast with those of a conventional catalyst prepared from H_2PtCl_6 and SnCl₂ precursors, indicating the relevance of the platinum precursor, which yields a definite Pt–Sn interaction. The synthesized silica-supported PtSn alloy is active in the RWGS reaction and in the catalytic reaction among CO_2, C_2H_4, and H_2O to give selectively lactic acid.

ACKNOWLEDGMENTS

REFERENCES

1. Dautzenberg, F. M., Helle, J. N., Biloen, P., and Sachtler, W. M. H., *J. Catal.* **63,** 119 (1980).
2. Burch, R., and Garla, L. C., *J. Catal.* **71,** 360 (1981).
3. Galvagno, S., Donato, A., Neri, G., Pietropaolo, R., and Poltarzewski, Z., *J. Mol. Catal.* **42,** 379 (1987).
4. Margitfalvi, J. L., Hegedüs, M., Tálas, E., *J. Mol. Catal.* **51,** 279 (1989).
5. Coq, B., Tijani, A., and Figueras, F., *J. Mol. Catal.* **71,** 317 (1992).
6. Sparks, D. E., Srinivasan, R., and Davis, B. H., *J. Mol. Catal.* **88,** 359 (1994).
7. Handy, B. E., Dumesic, J. A., Sherwood, R. D., and Baker, R. T. K., *J. Catal.* **124,** 160 (1990).
8. Chojnacki, T. P., and Schmidt, L. D., *J. Catal.* **129,** 473 (1991).
9. Srinivasan, R., Rice, L. A., and Davis, B. H., *J. Catal.* **129,** 257 (1991).
10. Srinivasan, R., and Davis, B. H., *Appl. Catal.* **87,** 45 (1992).
11. Srinivasan, R., and Davis, B. H., *Platinum Met. Rev.* **36,** 151 (1992).
12. Homs, N., Clos, N., Muller, G., Sales, J., and Ramírez de la Piscina, P., *J. Mol. Catal.* **74,** 401 (1992).
13. Ramírez de la Piscina, P., Fierro, J. L. G., Muller, G., Sales, J., Homs, N., *Catal. Lett.* **14,** 45 (1992).
14. Llorca, J., Ramírez de la Piscina, P., Sales, J., and Homs, N., *J. Chem. Soc. Chem. Commun.,* 2555 (1994).
15. Cavinato, G., and Toniolo, L., *Inorg. Chim. Acta* **52,** 39 (1981).
16. Wagner, C. D., Davis, L. E., Zeller, M. V., Taylor, J. A., Raymond, R. H., and Gale, L. H., *Surf. Interface Anal.* **3,** 211 (1981).